

# The Humidity Dependence of Pentacene Organic Metal-Oxide-Semiconductor Field-Effect Transistor

Fadliondi<sup>\*1</sup>, Muhammad Kunta Biddinika<sup>2</sup>, Shun-ichiro Ohmi<sup>3</sup>

<sup>1</sup>Teknik Elektro Universitas Muhammadiyah Jakarta, Jakarta, Indonesia

<sup>2,3</sup>Tokyo Institute of Technology, Tokyo

\*Corresponding author, e-mail: fadliondi@yahoo.com

## Abstract

*Metal-oxide-semiconductor field-effect transistors (MOSFET) were fabricated using organic semiconductor pentacene. The humidity dependence of drain current gate voltage ( $I_D$ - $V_G$ ) characteristic and drain current drain voltage characteristic ( $I_D$ - $V_D$ ) will be explained. Firstly, the thermal oxidation method was used to grow  $\text{SiO}_2$  gate insulator with thickness of 11 nm. Secondly, the thermal evaporation method was used to form Au source and drain electrodes with thickness of 28 nm. The channel width and length of the transistors were 500 nm and 200 nm, respectively. By the same method, organic semiconductor material pentacene was deposited with thickness of 50 nm at vacuum of  $7.8 \times 10^{-6}$  Torr. The hole mobility decreased from  $0.035 \text{ cm}^2/(\text{Vs})$  to  $0.006 \text{ cm}^2/(\text{Vs})$ , while the threshold voltage increased from 0.5 V to 2.5 V and gate leakage current also increased from  $5.8 \times 10^{-10}$  A to  $3.3 \times 10^{-9}$  A when the relative humidity increased from 20% to 70%.*

**Keywords:** pentacene, semiconductor, organic, electronics, transistor

Copyright © 2017 Universitas Ahmad Dahlan. All rights reserved.

## 1. Introduction

Organic electronic devices have become attraction due to their low-cost, low-temperature process and flexibility [1]. Organic thin-film transistors have been applied applications in displays and flexible electronic devices [2]. Organic thin-film transistors can also be applied for biological and chemical sensors. The advantages of organic thin-film transistor are fine tuning of their electrical properties, low-temperature fabrication, low-cost fabrication, on-large-area fabrication and flexibility. Decreasing the size of transistors can increase current and switching speed. In organic thin-film transistors, decreasing the number of grain boundaries can increase the effective mobility. They are fabricated using either thermal evaporation method or spin-coating method. To obtain better characteristics, there are many factors that should be improved like gate capacitance, interfacial between semiconductor and source drain electrode and the orientation of semiconductor layer. There has been a laboratory group who has developed inverter using MOSFET fabricated from organic semiconductor even though parameters like low gain, high power dissipation and high operating voltage need to be improved [3]. One of semiconductor materials widely used is pentacene. Pentacene has become attention because of its availability, device performance and environment stability. Pentacene is a commonly-studied organic semiconductor having mobility close to amorphous silicon for organic thin-film transistors and pentacene is deposited using thermal evaporation method [4]. The pentacene transistors devices characteristic is sensitive to the property of its dielectric, source drain electrodes, impurity, and substrate temperature and deposition rate. Pentacene MOSFET can have hole mobility from  $0.01 \text{ cm}^2/(\text{Vs})$  to  $1 \text{ cm}^2/(\text{Vs})$ . Field-effect transistors based on organic semiconductor have good performance appropriate for electronic devices industry. Because pentacene is an organic semiconductor material, it is very sensitive to humidity. Therefore, pentacene can be applied for humidity sensor [5, 6]. Pentacene can also be applied for ferroelectric organic field-effect transistor [7].

## 2. Research Method

As gate insulator layer,  $\text{SiO}_2$  with thickness of 11 nm was grown using the thermal oxidation method. Pentacene deposited on thermal oxidation  $\text{SiO}_2$  has better hole mobility and

larger crystal size than that deposited on plasma enhanced chemical vapor deposition (PECVD)  $\text{SiO}_2$  [8]. Next, by the thermal evaporation method, Au source and drain electrodes were formed with thickness of 28 nm. Then, pentacene semiconductor layer with thickness of 53 nm was deposited using the same method at room temperature and at vacuum of  $7.8 \times 10^{-6}$  Torr. Pentacene deposited using thermal evaporation method has better uniformity and thinner layer than that deposited using spin-coating method. Au (gold) has almost the same Fermi level with the highest occupied molecular orbital (HOMO) of pentacene, so hole carrier injection become easier [9]. The channel width and length of the transistors were 500  $\mu\text{m}$  dan 200  $\mu\text{m}$  respectively. Finally, electrical characteristics measurement and XRD measurement were carried out.

### 3. Results and Analysis

Figure 1 shows the measurement method. **Error! Reference source not found.** shows the humidity dependence of drain current drain voltage characteristics. The horizontal axis and vertical axis represent drain voltage and drain current respectively. The RH is relative humidity. The  $V_G$  is gate voltage. When the relative humidity increased from 20% to 70%, the absolute value of drain current at  $V_{DS} = V_G = -5$  V decreased from 0.45 mA to 0.13 mA. The drain current decreased because the hole mobility decreased.

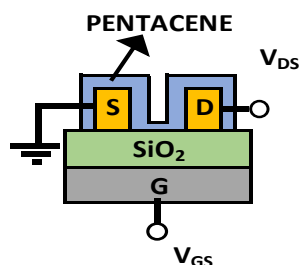


Figure 1. Measurement point.

Figure 3 shows the humidity dependence of drain current gate voltage characteristic. The horizontal and vertical axes represent gate voltage and drain current, respectively. The drain voltage was fixed at -5V. When the relative humidity increased from 20% to 70%, the current decreased from  $4.5 \times 10^{-7}$  A to  $1.3 \times 10^{-7}$  A. Higher applied drain voltage was not applied because the gate insulator was very thin as much as 11 nm. Carrier-injection hysteresis could be seen at Figure 3.

Figure 4(a) shows the humidity dependence of threshold voltage. The left and right vertical axis represents the normalized current and the threshold voltage respectively. The horizontal axis represents the relative humidity. Figure 4(a) shows that the threshold voltage increased from 0.5 V to 2.5 V when the relative humidity increased from 20% to 70%. Figure 4(b) shows the humidity dependence of the hole mobility and off current. The left and right horizontal axes represent the hole mobility and off current respectively. Figure 4(b) shows that the hole mobility of pentacene decreased from  $0.035 \text{ cm}^2/(\text{Vs})$  to  $0.006 \text{ cm}^2/(\text{Vs})$  and the off current increased from  $5.8 \times 10^{-10}$  A to  $3.3 \times 10^{-9}$  A when the relative humidity increased from 20% to 70%. The hole mobility of pentacene decreased due to polar water molecules [10-13]. Water molecules residing at grain boundaries interact with holes charge carriers reducing the mobility of charge carrier [10-13]. The diffusion of water molecules into grain boundaries changes the interactions among molecules increasing the barrier energy for transportation of charge carrier among grains [10-13]. These mechanisms lead to decreasing on current and mobility on organic field-effect transistors. The threshold voltage increases because mobile charges are induced into semiconductors by water vapor [10-13]. The larger positive gate voltages are needed to compensate holes on the channel to turn off the transistors [10-13]. The on current at large negative voltage decreases due to decreasing hole mobility [10-13]. The decreasing saturation current is the indication of charge transport limited by grain boundaries. The off current increases because mobile charges are induced at semiconductor layer by water vapor [10-13].

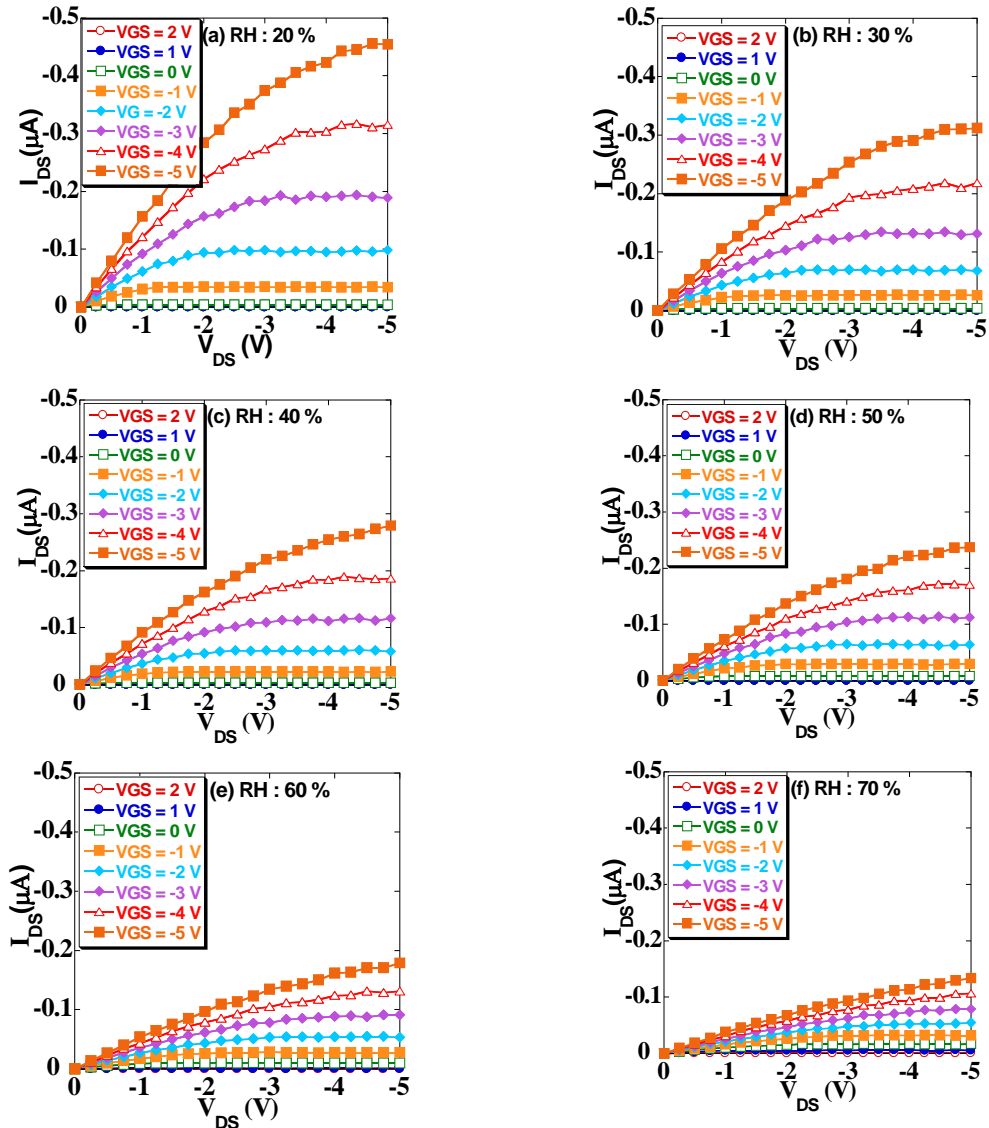


Figure 2. The humidity dependence of  $I_D$ - $V_D$  characteristics (a) 20%, (b) 30%, (c) 40%, (d) 50%, (e) 60%, (f) 70%

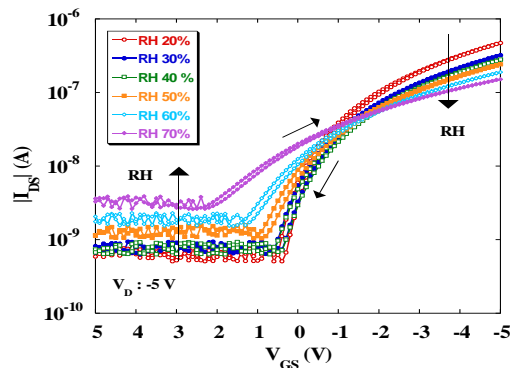


Figure 3. The humidity dependence of  $I_D$ - $V_G$  characteristics

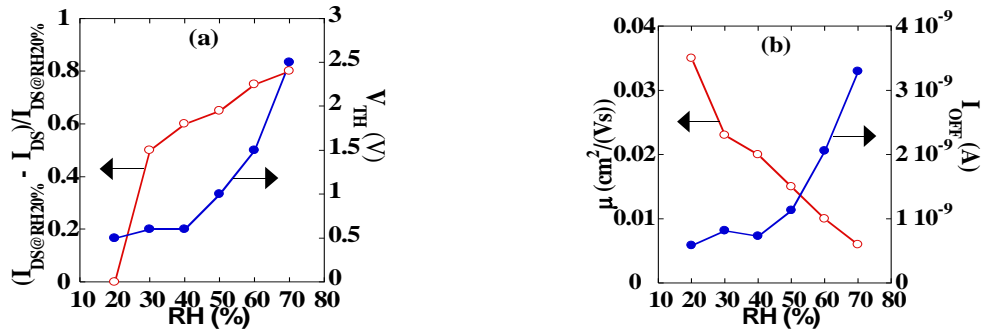


Figure 4. The humidity dependence of (a) on current, threshold voltage, (b) hole mobility and off current

Figure 5(b) shows that  $I_{ds}$  reaches the 20% RH level after pumping the moisture. When the relative humidity is around 20%, the drain current magnitude reaches around  $0.46 \mu\text{A}$ . When the humidity is increased to level of 60%, the drain current magnitude drops significantly to around 0.2 mA. When the moisture is pumped out and the relative humidity reaches 20%, the drain current magnitude reaches around 0.45 mA. This indicates that the change in the saturation current is reversible. However the reversibility seems to degrade by time. The Equation (1) shows the main equations for p-channel MOSFET. Cut-off region is a condition when the resistance between drain and source is maximum so very small current or no current flows between drain and source. Linear region is a condition when the transistor is on and the channel is formed so current can flow between source and drain. Saturation region is a condition when the transistor is on and the channel is formed, but drain current is no longer dependent on drain voltage and is mainly controlled by gate voltage.  $W$  and  $L$  are the channel width and length respectively.  $C_{ox}$  is gate oxide capacitance and  $m$  is mobility.

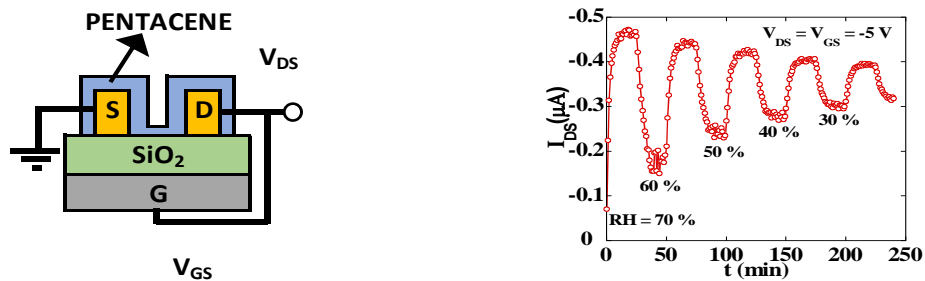


Figure 5. (a) measurement point (b) time dependence of saturation current

$$I_{SD} = \begin{cases} 0 & \text{when } V_{SG} \leq |V_{TH}| \quad (\text{cut off}) \\ \frac{\mu C_{ox} W}{L} \left[ V_{SG} - |V_{TH}| V_{SD} - \frac{V_{SD}^2}{2} \right] & \text{when } V_{SG} > |V_{TH}| \text{ and } V_{SD} \leq V_{SG} - |V_T| \quad (\text{linear}) \\ \frac{\mu C_{ox} W}{L} \left[ \frac{(V_{SG} - |V_{TH}|)^2}{2} \right] & \text{when } V_{SG} > |V_{TH}| \text{ and } V_{SD} > V_{SG} - |V_{TH}| \quad (\text{saturation}) \end{cases} \quad (1)$$

$$SS = \frac{dV_{GS}}{d(\log I_{DS})} \quad (2)$$

$$D_{it} = \left[ \frac{SS}{\frac{kT}{e} \ln 10} - 1 \right] \frac{C_{ox}}{e^2} \quad (3)$$

$$R_s = \frac{I_{DS}}{V_{DS}} - \frac{L}{WC_{ox}\mu(V_{GS} - V_{TH})} \tag{4}$$

Figure 6 shows the humidity dependence of  $V_{on}$  and subthreshold swing. The left and right vertical axis represents the  $V_{on}$  and the subthreshold swing respectively. The horizontal axis represents the relative humidity. Figure 6(a) shows that the  $V_{on}$  increased from 0.7 V to 2.7 V and subthreshold swing increased from 0.4 V/dec to 8 V/dec when the relative humidity increased from 20% to 70%. Figure 6(b) shows the humidity dependence of series resistance and interface trap density. The left and right horizontal axes represent the series resistance and interface trap density, respectively. Figure 6(b) shows that the series resistance decreased from 13 MW to 56.5 MW and the interface trap density increased  $1.1 \times 10^{13} \text{ cm}^2 \text{ eV}^{-1}$  to  $2.6 \times 10^{14} \text{ cm}^2 \text{ eV}^{-1}$  when the relative humidity increased from 20% to 70%. The subthreshold swing (SS) is calculated using Equation (2) where  $V_{GS}$  and  $I_{DS}$  are gate source voltage and gate source drain, respectively [14]. The interface trap density ( $D_{it}$ ) is calculated using Equation (3) where  $k$  is Boltzman constant,  $T$  is temperature,  $e$  is electron charge,  $C_{ox}$  is gate insulator capacitance [15, 16]. The series resistance ( $R_s$ ) is calculated using Equation (4) where  $m$  is hole mobility [17]. Table 1 shows the comparison with other works:

Table 1. Comparison with other works

Parameters	This work	Ref. 14
Structure	Bottom-contact	Top-contact
Gate	n <sup>+</sup> -Si	p <sup>+</sup> -Si
Gate insulator	SiO <sub>2</sub>	SiO <sub>2</sub>
Gate insulator thickness	11 nm	300 nm
Organic semiconductor	Pentacene	Pentacene
Organic semiconductor thickness	50 nm	40 nm
Channel length	200 mm	50 mm
Channel width	500 mm	3760 mm
Applied drain voltage	-5 V	-70 V
Applied gate voltage	-5 V	-40 V
Threshold voltage	0.5 V at RH 20% 1.5 V at RH 60%	29.8 V at RH 3% 67 V at RH 57%
	*RH : Relative Humidity	
Series resistance	13 MW at RH 20% 38.4 MW at RH 60%	9.34 MW at vacuum 4.22 MW at RH 57%
Subthreshold swing	0.4 V/dec at RH 20% 2.9 V/dec at RH 60%	2.61 V/dec at RH 3% 19.75 V/dec at RH 57%
Interface trap density	$1.11 \times 10^{13} \text{ cm}^2 \text{ eV}^{-1}$ at RH 20% $9.23 \times 10^{13} \text{ cm}^2 \text{ eV}^{-1}$ at RH 60%	$3.09 \times 10^{12} \text{ cm}^2 \text{ eV}^{-1}$ at RH 3% $2.38 \times 10^{13} \text{ cm}^2 \text{ eV}^{-1}$ at RH 57%
Mobility	$0.035 \text{ cm}^2/(\text{Vs})$ at RH 20% $0.010 \text{ cm}^2/(\text{Vs})$ at RH 60%	$0.0050 \text{ cm}^2/(\text{Vs})$ at RH 3% $0.0025 \text{ cm}^2/(\text{Vs})$ at RH 57%
$V_{on}$	0.7 V at RH 20% 1.8 V at RH 60%	56.2 V at RH 3% 60 V at RH 57%

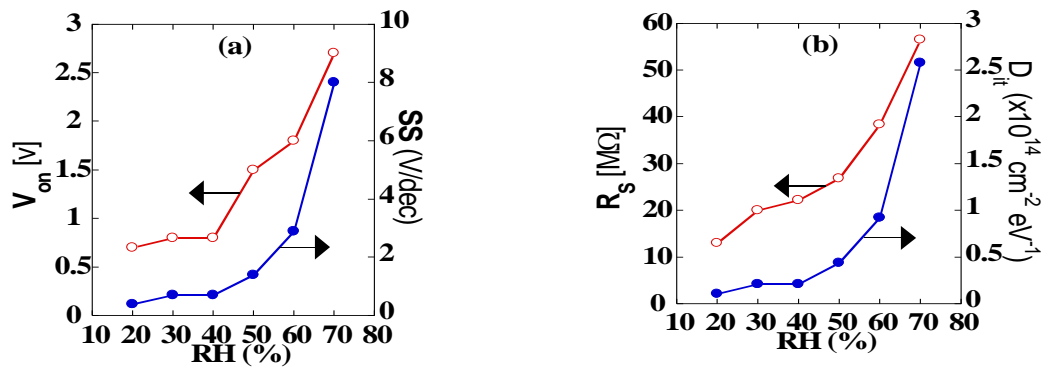


Figure 6. The humidity dependence of (a)  $V_{on}$ , subthreshold swing, (b) series resistance, interface trap density

#### 4. Conclusion

Metal-oxide-semiconductor field-effect transistors (MOSFET) were fabricated using organic semiconductor pentacene. The hole mobility decreased from  $0.035 \text{ cm}^2/(\text{Vs})$  to  $0.006 \text{ cm}^2/(\text{Vs})$ , while the threshold voltage increased from 0.5 V to 2.5 V and gate leakage current also increased from  $5.8 \times 10^{-10} \text{ A}$  to  $3.3 \times 10^{-9} \text{ A}$  when the relative humidity increased from 20 % to 70%.

#### References

- [1] Chang Hyun Kim, Omid Yaghmazadeh, Denis Tondelier, Yong Bin Jeong, Yvan Bonnassieux, and Gilles Horowitz. Capacitive behavior of pentacene-based diodes: Quasistatic dielectric constant and dielectric strength. *Journal of Applied Physics*. 2011; 109(8).
- [2] Hsiao-Wen Zana, Kuo-Hsi Yena, Pu-Kuan Liua, Kuo-Hsin Kuc, Chien-Hsun Chen, Jennchang Hwang. Low-voltage organic thin film transistors with hydrophobic aluminum nitride film as gate insulator. *Organic Electronics*. 2007; 8(4): 450-454.
- [3] Chia-Yu Wei, Wen-Chieh Huang, Chih-Kai Yang, Yen-Yu Chang, and Yeong-Her Wang. Low-Operating-Voltage Pentacene-Based Transistors and Inverters With Solution-Processed Barium Zirconate Titanate Insulators. *IEEE Electron Device Letters*. 2011; 32(12): 1755-1757.
- [4] Tapendu Mandal, Ashish Garg, and Deepak. Thin film transistors fabricated by evaporating pentacene under electric field. *Journal of Applied Physics*. 2013; 114(15).
- [5] Zheng-Tao Zhu, Jeffrey T Mason, Rüdiger Dieckmann, and George G Malliaras. Humidity sensors based on pentacene thin-film transistors. *Applied Physics Letters*. 2002; 81(24): 4643-4645.
- [6] Jacques Tardy, Mohsen Erouel. Stability of pentacene transistors under concomitant influence of water vapor and bias stress. *Microelectronics Reliability*. 2013; 53(2): 274-278.
- [7] Huabin Sun, Yao Yin, Qijing Wang, Qian Jun, Yu Wang, Kazuhito Tsukagoshi, Xizhang Wang, Zheng Hu, Lijia Pan, Youdou Zheng, Yi Shi, and Yun Li. Reducing contact resistance in ferroelectric organic transistors by buffering the semiconductor/dielectric interface. *Applied Physics Letters*. 2015; 107(5).
- [8] D Knipp, RA Street, B Krusor, R Apte, J Ho. Polycrystalline pentacene thin films for large area electronic applications. *Journal of Non-Crystalline Solids*. 2002; 299-302(2): 1042-1046
- [9] Akichika Kumatani, Yun Li, Peter Darmawan, Takeo Minari and Kazuhito Tsukagoshi. On Practical Charge Injection at the Metal/Organic Semiconductor Interface. *Scientific Reports*. 2013; 3(1026): 1-6.
- [10] Dawen Li, Evert-Jan Borkent, Robert Nortrup, Hyunsik Moon, Howard Katz, and Zhenan Bao. Humidity effect on electrical performance of organic thin-film transistors. *Applied Physics Letters*. 2005; 86(4).
- [11] H Dunlap, PE Parris, and VM Kenkre. Charge-Dipole Model for the Universal Field Dependence of Mobilities in Molecularly Doped Polymers. *Phys. Rev. Lett*. 1996; 77(3): 542.
- [12] J Gundlach, TN Jackson, DG Schlom, and SF Nelson. Solvent-induced phase transition in thermally evaporated pentacene films. *Appl. Phys. Lett*. 1999; 74(22): 3302-3304.
- [13] Zou and T Tsutsui. Voltage shift phenomena introduced by reverse-bias application in multilayer organic light emitting diodes. *J. Appl. Phys*. 1951; 87(4): 2000.
- [14] LA Majewski, M Grell. Organic field-effect transistors with ultrathin modified gate insulator. *Synthetic Metals*. 2005; 151(2): 175-179.
- [15] G Horowitz. Tunneling Current in Polycrystalline Organic Thin-Film Transistors. *Advanced Functional Materials*. 2003; 13(1): 53-60.
- [16] Christopher R Newman, Daniel Frisbie, Demetrio A da Silva Filho, Jean-Luc Brédas, Paul C Ewbank and Kent R Mann. Introduction to Organic Thin Film Transistors and Design of n-Channel Organic Semiconductors. *Chem. Mater*. 2004; 16(23): 4436-4451.
- [17] Gilles Horowitz, Riadh Hajlaoui, Denis Fichou, Ahmed El Kassmi. Gate voltage dependent mobility of oligothiophene field-effect transistors. *Journal of Applied Physics*. 1999; 85(6): 3202-3206.
- [18] W Boukhili, M Mahdouani, M Erouel, J Puigdollers, R Bourguiga. Reversibility of humidity effects in pentacene based organic thin-film transistor: Experimental data and electrical modeling. *Synthetic Metals*. 2015; 199: 303-309.